



Article

Soil and Water Losses with Simulated Rainfall Considering Experimental Plots and Rainfall Patterns

Daniel Fonseca de Carvalho ^{1,*}, Amanda Sales Alves ², Pietro Menezes Sanchez Macedo ²,
Paulo Tarso Sanches de Oliveira ³ and Nivaldo Schultz ⁴

¹ Department of Engineering, Institute of Technology, Federal Rural University of Rio de Janeiro, Seropédica 23897-000, Rio de Janeiro, Brazil

² Postgraduate Program in Agronomy-Soil Sciences, Federal Rural University of Rio de Janeiro, Seropédica 23897-000, Rio de Janeiro, Brazil; amandasalesalves@ufrj.br (A.S.A.); emagenao@gmail.com (P.M.S.M.)

³ Faculty of Engineering, Architecture and Urbanism and Geography, Federal University of Mato Grosso do Sul, Campo Grande 79070-900, Mato Grosso do Sul, Brazil; paulo.t.oliveira@ufms.br

⁴ Department of Soil Science, Institute of Agronomy, Federal Rural University of Rio de Janeiro, Seropédica 23897-000, Rio de Janeiro, Brazil; nivaldods@ufrj.br

* Correspondence: carvalho@ufrj.br; Tel.: +55-(21)-98787-7262

Abstract: Rainfall simulators are important pieces of equipment to investigate hydrological processes and soil erosion. Here, we investigated the operational characteristics, the rainfall characteristics, and the soil erosion process under collecting plots and rainfall patterns using the *InfiAsper* simulator. We evaluated the standard plot of the simulator in a rectangular shape (1.0 × 0.7 m), as well as a circular plot (0.8 m diameter), and four precipitation patterns, characterized as advanced (AV), intermediate (IN), delayed (DL), and constant (CT). In the laboratory, uniformity and water consumption tests were carried out for shutter-disk rotations from 138 to 804 rpm, and in the field, simulated rains were applied on a Dystric Acrisol. Rains with different patterns were simulated and presented a uniformity coefficient above 83% for the circular plot and 78.2% for the rectangular plot. The soil erosion varied as a function of the precipitation patterns and, to a lesser extent, according to the shape of the experimental plot. However, runoff and soil loss in AV were 2.1 and 3.5 times greater when using a circular plot. Concerning IN and DL, the length of the rectangular plot may have influenced the formation of small furrows throughout most of the simulated rainfall event, providing greater runoff (13.1 mm) and soil loss (13.6 g m⁻²). The results obtained are promising, but plots with different shapes associated with rainfall patterns simulated by *InfiAsper* must be evaluated in other classes and soil use and cover conditions.

Keywords: soil erosion; runoff collecting plots; rainfall uniformity; precipitation intensity; *InfiAsper* rainfall simulator



Citation: de Carvalho, D.F.; Alves, A.S.; Macedo, P.M.S.; de Oliveira, P.T.S.; Schultz, N. Soil and Water Losses with Simulated Rainfall Considering Experimental Plots and Rainfall Patterns. *Soil Syst.* **2023**, *7*, 87. <https://doi.org/10.3390/soilsystems7040087>

Academic Editor: Adriano Sofó

Received: 13 July 2023

Revised: 5 October 2023

Accepted: 13 October 2023

Published: 17 October 2023



Copyright: © 2023 by the authors. Licensee MDPI, Basel, Switzerland. This article is an open access article distributed under the terms and conditions of the Creative Commons Attribution (CC BY) license (<https://creativecommons.org/licenses/by/4.0/>).

1. Introduction

Rainfall simulators are devices designed for sprinkling water similarly to natural rainfall to facilitate studies on water erosion, surface runoff, and water infiltration into the soil [1–4]. These pieces of equipment have been used to evaluate the erosion process under laboratory conditions [5] and in the experimental field [6–8]. Concerning studies on natural rainfall, they have advantages such as the ability to reproduce rainfall events with similar characteristics, the possibility of varying the diameter and kinetic energy of the drops [9], and reducing the time and costs involved in conducting research [10].

The choice of a rainfall simulator must be made according to some aspects, such as portability, simplicity of operation, uniform rainfall distribution, easy handling and speed of operation, water consumption, and the relationship between simulated and natural rainfall kinetic energy [11,12]. Despite the aforementioned advantages and applications, not all

simulators allow for the variation of precipitation intensity (PI) during rain applications [13], a natural characteristic of rainfall events [14]. The variation of PI throughout the event allows the reproduction of different rainfall patterns, which are characterized according to the occurrence of peak precipitation in relation to the duration of the rain, which may influence the soil erosion process [15].

The *InfiAsper* simulator [16] meets the requirements mentioned above and has been used in various soil and water management and conservation studies carried out in Brazil [17–19]. The equipment is classified as a rotating disk [20] and was developed to apply rainfall with constant PI, ranging from 20 to 150 mm h⁻¹ and with uniformity greater than 75%, using an experimental plot of 0.70 m². To overcome the limitation of applying rainfall with constant intensity, allowing the simulation of different precipitation patterns, Macedo et al. [21] developed a new control panel for the *InfiAsper*, making it possible to vary the intensity of the rainfall during applications by regulating the shutter-disc rotation, thus reproducing the natural soil loss process more efficiently [22].

Water distribution uniformity is crucial for rainfall simulators [23] and is often evaluated by the Christiansen Uniformity Coefficient (CU) [24]. Several authors recommend reference values for CU in studies with simulated rainfall, although even the uniformity of natural rainfall is very variable due to the complexity of the micro-physical variables involved [25]. Using the new control panel, Macedo et al. [21] evaluated the *InfiAsper* operating with different rainfall patterns and achieved uniformities varying from 76.9% to 79.4%, and the relationship between simulated and natural kinetic energy was predominantly greater than 80% for different rainfall patterns.

Increasing simulated rainfall uniformity provides better results in studies related to water erosion, which depends on the shape and size of the experimental plot [26] responsible for conditioning the surface runoff. Experimental plots of different areas and shapes used in rainfall simulators are reported in the literature. Amore et al. [27] highlights that it is important to consider the effect of the experimental plot in the soil erosion estimation, in addition to other variables such as soil tillage and management and soil type. For instance, Iserloh et al. [11] evaluated the rainfall characteristics of 13 rainfall simulators, of which 8 had circular plots, 4 rectangular, and 1 trapezoidal, with an area ranging from 0.159 to 1.0 m². The authors concluded that the effects of experimental plot designs on runoff and soil erosion processes should be evaluated, especially under simulated rainfall. To the best of our knowledge, there are no studies evaluating the effects of experimental plot designs and considering rainfall with the same characteristics (intensity, duration, and kinetic energy). Therefore, the main objective of this study is to evaluate the effect of the shape and area of an experimental plot on rainfall distribution and soil erosion processes. To do this, we used rainfall patterns obtained by the *InfiAsper* simulator using rectangular 0.70 m² (RP) and circular plots (CP) of 0.50 m², for which consumption (CW), water use efficiency (WUE), and the rain uniformity coefficient (CU) were evaluated for different operating conditions of the rain simulator.

2. Materials and Methods

2.1. Rainfall Simulator Description

We used the *InfiAsper* rainfall simulator [16] (Figure 1), operating with a 1.0 hp motor pump. The rainfall is controlled via a control panel that activates the motor pump and controls the shutter-disc rotation using a frequency inverter. The simulator operates with two Veejet 80.150 nozzles parallel to each other, positioned 2.3 m from the ground surface. The mean diameter of drops applied by the simulator is around 2.0 mm, considering the different pressure settings. In this study, the opening of the shutter disc was maintained at 56 mm and the water pressure at 27.6 kPa, values defined from previous evaluations. We used the new control panel that allows the precipitation intensity (PI) to be varied and the rainfall to be programmed based on pre-defined patterns proposed by [21].



Figure 1. Description of the components of the *InfiAsper* rainfall simulator (Legend: metallic structure (1); water application unit (2); control panel (3); water reservoir (4); water pump (5); and runoff collector (6)).

Figure 2a shows the usual rectangular runoff collection plot of the *InfiAsper*, with an area of 0.7 m^2 ($1.0 \times 0.7 \text{ m}$). Here, we proposed a circular experimental plot (Figure 2b), defined according to the simulator's spraying shape. Due to its operational characteristics, the area wetted by the *InfiAsper* has a smaller dimension in the transverse direction to the runoff, with just over 0.80 m . Therefore, the circular plot was built with 0.80 m and 0.5 m^2 of diameter and area, respectively. Galvanized steel sheets were used to construct plots of both shapes with a height of 0.25 m . These plots were driven into the ground and positioned about 0.02 m above the soil surface.



Figure 2. Rectangular (a) and circular (b) plots used in the study.

2.2. Experimental Procedure

We divided this study into two experimental steps: laboratory and field. First, in the laboratory, we evaluated both the uniformity using the CU (Equation (1)) and the PI in tests with disk rotations of 138, 264, 420, 684, and 804 rpm and a duration of 5 min.

$$CU = 1 - \frac{\sum_{i=1}^n |X_i - \bar{X}|}{n \bar{X}} \quad (1)$$

where:

X_i —rainfall depth in each collector (mm);

\bar{X} —mean rainfall depth (mm);

n —number of collecting bottles.

The water consumption (WC) of the *InfiAsper* at different disc rotations was also evaluated by collecting and measuring the water volume applied. From there, we obtained the efficiency of the equipment (WUE), which was obtained from the ratio between the volume collected in the plots and the WC.

For each simulated rainfall test, totaling 5 repetitions per rotation, the applied water was collected in plastic containers, 50 cm² in area, distributed inside the plot, using a graduated cylinder measuring 1.0 mm to measure the volume. Ninety-two collectors were used in the rectangular plot and 81 in the circular plot, allowing the calculation of uniformity and the spatial distribution of rainfall. Based on these results, models relating PI with rotation were adjusted for rectangular and circular plots, enabling the operation of *InfiAsper* with instantaneous variations of PI during tests with simulated rainfall. Flanagan et al. [15] classified rainfall patterns according to the moment of occurrence of the precipitation peak in relation to the rainfall duration. In the Advanced (AV), Intermediate (IN), and Delayed (DL) patterns, the PI peak occurs in the initial, middle, and final third of the rainfall, respectively, and may influence the erosion process due to the water content in the surface layer of the soil.

From the calibration curves, the AV, IN, and DL patterns were programmed for each plot, considering a mean PI of 45 mm h⁻¹ and a duration of 40 min, with PI varying from 30 to 110 mm h⁻¹, according to the methodology presented by [21]. In addition, tests with constant (CT) precipitation intensity were also performed. Therefore, the kinetic energy varied from 11.20 to 41.08 J m⁻² min⁻¹, according to the computational routine presented by [16].

The rainfalls were simulated using the information from each pattern, which was constantly recorded (every minute) in a txt file on a microSD card that was later accessed by the *InfiAsper* control panel. The rainfall uniformity and spatial distribution with the different patterns were also evaluated for the two collecting experimental plots using the same methodology mentioned above.

After the laboratory tests, the second step was carried out in the field, where soil loss and surface runoff were evaluated in a ploughed and harrowed area of an ARGISSOLO VERMELHO-AMARELOS Distrófico (Dystric Acrisol according to the World Reference Base for Soil Resources) [28] with a loamy sand texture (0.0–0.34 m). This area had been uncultivated for at least 2 years, and Table 1 shows its granulometric composition and the soil physical attributes in the different horizons. Soil organic carbon was evaluated in the 0.0–0.18 m layer, indicating 20.82 g kg⁻¹.

Table 1. Physical attributes and granulometric composition of a Dystric Acrisol in the different horizons.

Horizon *	PD	BD	TP	Ks	Sand			Silt	Clay
					Coarse	Fine	Total		
	(g cm ⁻³)		(%)	(m h ⁻¹)			(%)		
Ap (0.0–0.18 m)	2.38	1.64	31.10	0.0358	66	17	83	4	13
A (0.18–0.34 m)	2.42	1.57	35.17	0.0629	64	17	81	8	11
AB (0.34–0.41 m)	2.29	1.58	31.23	0.0489	56	16	72	8	20
BA (0.41–0.51 m)	2.26	1.72	24.17	0.0671	42	11	53	9	38
Bt1 (0.51–0.92 m)	2.06	1.45	29.86	0.0782	28	4	32	16	52

* The soil horizon/layer names' are in accordance with the Brazilian Soil Classification System [29]. PD—particle density; BD—bulk density; TP—total porosity; Ks—hydraulic conductivity of the saturated soil; Coarse sand (0.2 to 2.0 mm); fine sand (0.05 to 0.2 mm); total sand (2–0.05 mm); silt (0.05–0.002 mm); clay (<0.002 mm).

A randomized block design was adopted in a 2 × 4 factorial scheme (2 plot shapes × 4 rainfall patterns), resulting in a total of eight treatments with four replications. The treatments

corresponded to the surface-runoff collecting plots (rectangular and circular) and to the four rainfall patterns (CT, AV, IN, and DL), totaling 32 experimental plots.

The area had a mean slope of 0.09 m m^{-1} , and once installed, the plots were pre-wet and close to the surface using a watering can, aiming to standardize the soil moisture in the respective experimental units and reduce the time between the beginning of the precipitation and the surface runoff [10]. Then, the *InfiAsper* simulator was installed and positioned to apply rainfall, maintaining a height of 2.3 m from the nozzles to the ground surface. The metallic structure of the rainfall simulator permits the adjustment of rods to maintain the obturator disc in a horizontal position, while the runoff collector outlet is positioned in the direction of the slope (see Figure 1).

Surface runoff and soil loss were assessed by collecting the runoff volume from each plot. Samples were collected at one-minute intervals from the start of the runoff, and the water volume was quantified using a 1000-mL measuring cylinder. Soil loss was estimated by determining the sediment runoff weight per sample after drying the material in an oven at $60 \text{ }^\circ\text{C}$.

2.3. Statistical Analysis

The data were submitted to the Shapiro–Wilk test to check the normality of the residuals, followed by an analysis of variance (ANOVA). Tukey’s test was then applied at 5% probability to compare the mean values. The statistical analysis was carried out using the SISVAR 5.7 software [30].

3. Results

3.1. Precipitation Intensity, Water Use Efficiency, and the Uniformity Coefficient

Changes in the rotation of the rainfall simulator’s motor affect the volume of water passing through the disk apertures. Therefore, the increase in disk rotation provides a reduction in the WC of the *InfiAsper* simulator and, consequently, in PI. However, we noted a higher range of PI values in the circular than in the rectangular plots (Table 2). The circular plot provided an increase in the uniformity coefficient of the simulated rainfall by the *InfiAsper* in relation to the rectangular plot. For the different rotations, CU ranged from 90.3% to 75.8% in the circular plot and from 82.5% to 67.5% in the rectangular plot, reaching the highest values at 420 rpm for the circular plot and 264 rpm for the rectangular plot.

Table 2. Water consumption (WC), precipitation intensity (PI), water use efficiency (WUE), and uniformity coefficient of the simulated rainfall (CU) in the circular plot and rectangular *InfiAsper* plot.

Rotation (rpm)	WC (L min^{-1})	Circular Plot			Rectangular Plot		
		PI (mm h^{-1})	WUE (%)	CU (%)	PI (mm h^{-1})	WUE (%)	CU (%)
138	2.24	146.4	54.4	84.9	114.9	59.5	81.2
264	1.61	99.5	51.6	89.3	80.8	58.4	82.5
420	1.19	75.7	53.0	90.3	62.1	60.6	81.0
684	0.58	34.3	49.3	83.0	35.4	71.0	72.2
804	0.50	26.7	44.3	75.8	28.2	65.1	67.5

3.2. Characterization of the Rainfall Patterns

From the PI and rotation data shown in Table 2, calibration curves were generated for each shape of the studied plot (Figure 3), which are considered essential for obtaining precipitation patterns. The simulated rainfall under different patterns was programmed according to Figure 4, with a duration of 40 min, a total depth of 30 mm, and a PI peak of 110 mm h^{-1} for each rainfall event. The disk rotation values were inserted in a text file for each minute and recorded on a micro-SD memory card [21]. The electronic system on the simulator’s control panel read this information and acted on the motor frequency inverter, changing the disc rotation and, consequently, the PI.

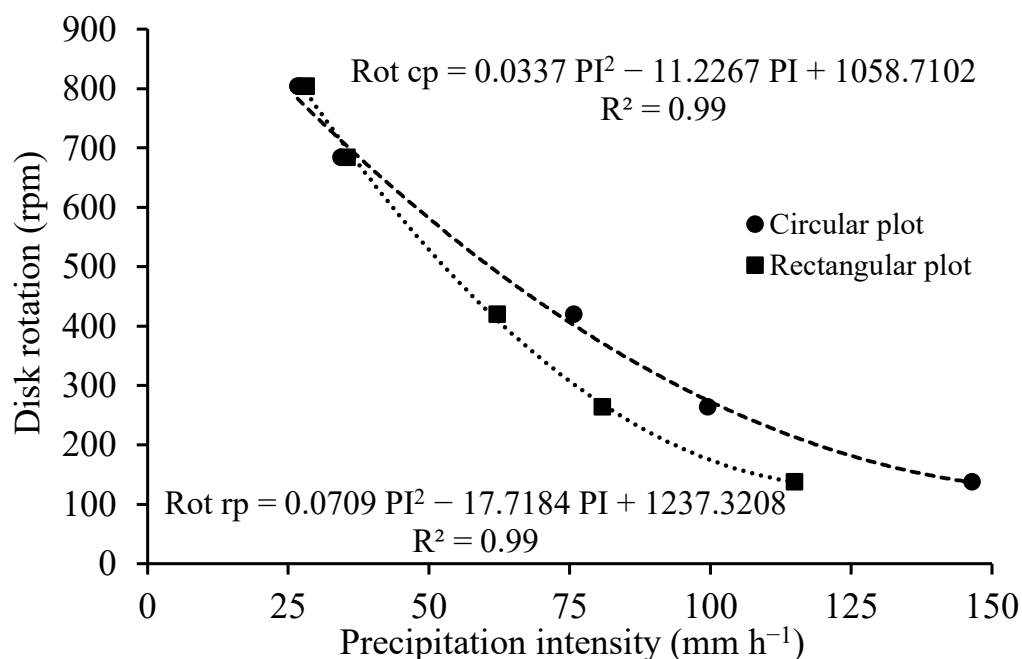


Figure 3. Calibration curve obtained in tests of five minutes duration in circular (cp) and rectangular (rp) experimental plots.

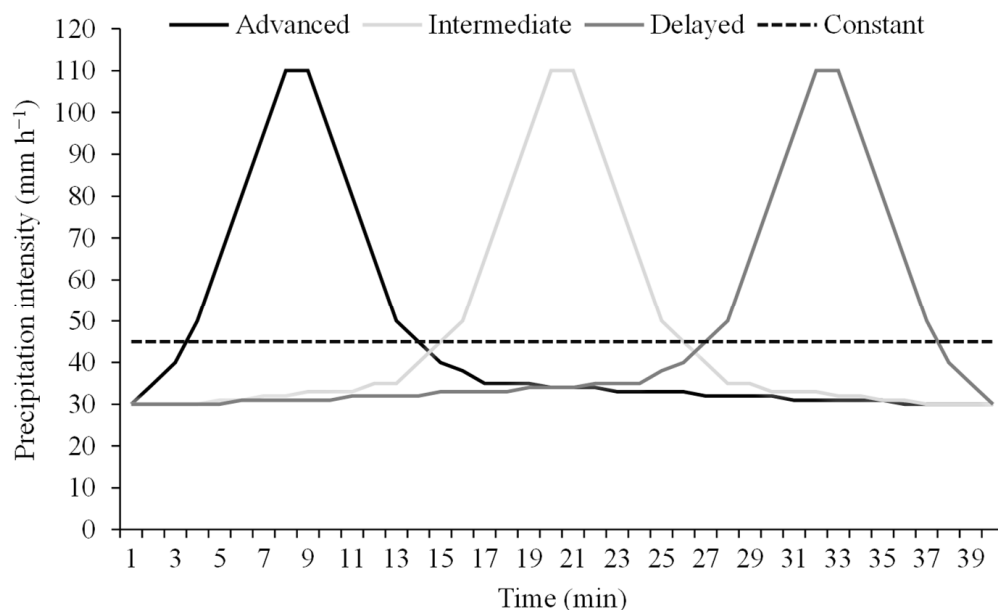


Figure 4. Rainfall patterns obtained with the rainfall simulator calibrated for tests lasting 40 min have a peak PI of 110 mm h⁻¹ and a rainfall depth of 30 mm.

3.3. Spatial Distribution of the Precipitation Intensity

The spatial distribution of PI varied between experimental plots (Figures 5 and 6). However, we did not find a significant difference between the rainfall patterns evaluated, indicating the quality of the calibration performed (Figure 3) and the satisfactory functioning of the new *InfiAsper* control panel proposed by [21].

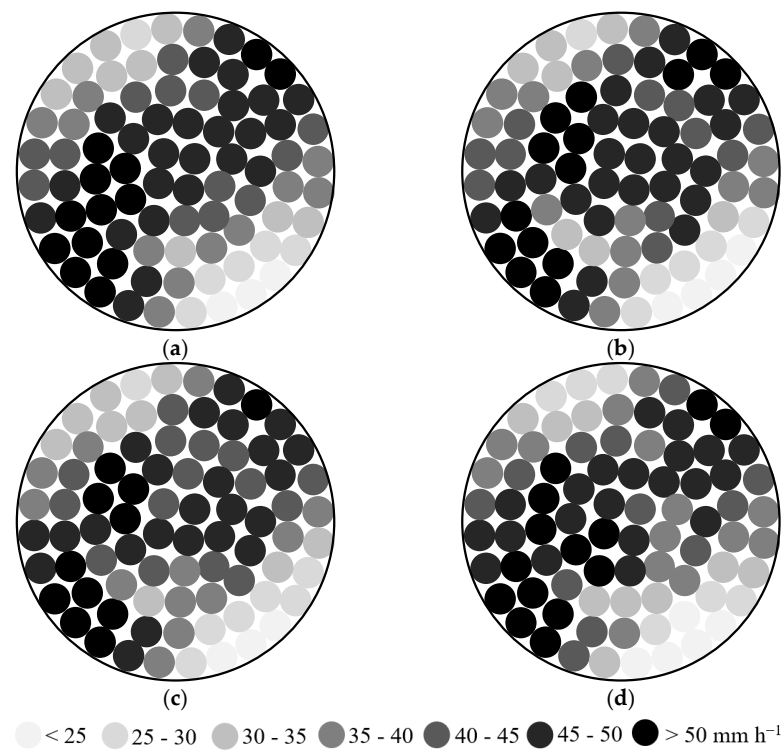


Figure 5. Spatial distribution of the PI of rainfall applied by the *InfiAsper* simulator for the advanced (a), intermediate (b), delayed (c), and constant (d) (mm h⁻¹) patterns in the circular plot.

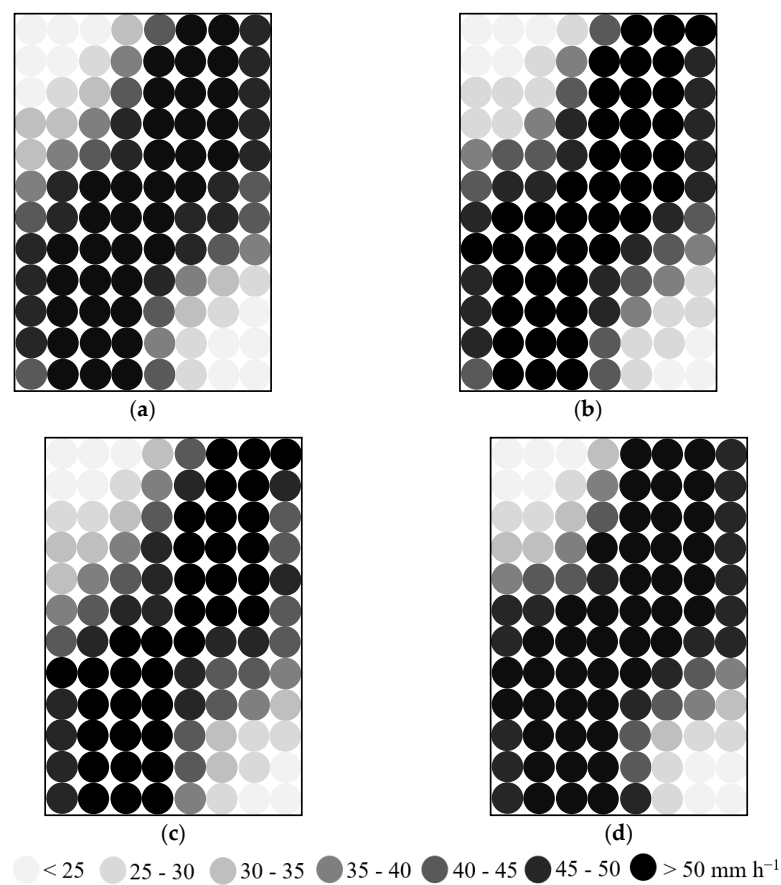


Figure 6. Spatial distribution of the PI of rainfall applied by the *InfiAsper* simulator for the advanced (a), intermediate (b), delayed (c), and constant (d) (mm h⁻¹) patterns in the rectangular *InfiAsper* plot.

In general, we found good uniformity for all the patterns in both shapes of plots, confirming the potential of using the *InfiAsper* simulator in water erosion studies (Table 3).

Table 3. Uniformity coefficients (%) for the different collecting plots and rainfall patterns.

Plots	Rainfall Patterns			
	Advanced	Intermediate	Delayed	Constant
Rectangular	78.2	79.0	78.5	77.7
Circular	83.5	83.8	83.5	81.7

3.4. Water and Soil Losses

The runoff and soil loss mean values varied as a function of the precipitation patterns and, to a lesser extent, according to the shape of the experimental plot (Table 4). For the AV pattern, the runoff depth in the circular plot was greater than that in the rectangular plot, while the opposite was noted for the DL pattern; a similar runoff depth was observed in both types of plots for the IN and CT patterns. Within each of the circular plots, the greatest values occurred with the AV and IN patterns, differing from CT, which showed the least runoff. For the rectangular plot, the IN and DL patterns showed the greatest runoff, differing from AV and CT, which presented less runoff. In the delayed pattern (DL), when the PI peak occurred after 33 min, the greater length of the rectangular plot may have favored the formation of small furrows throughout the simulated rainfall event (Figure 7), providing greater runoff (14.1 mm) and soil loss (14.1 g m⁻²).

Table 4. Runoff depth and soil loss in the circular and rectangular plots for different rainfall patterns lasting 40 min.

Rainfall Patterns	Runoff Depth (mm)		Soil Loss (g m ⁻²)	
	Circular Plot	Rectangular Plot	Circular Plot	Rectangular Plot
Advanced	14.4 ± 0.7 aA	6.7 ± 3.5 bB	27.2 ± 7.2 aA	7.8 ± 3.9 bAB
Intermediate	14.3 ± 2.0 aA	12.0 ± 1.1 aA	16.8 ± 0.9 aAB	13.1 ± 3.0 aA
Delayed	10.4 ± 2.7 bAB	14.1 ± 2.4 aA	10.6 ± 1.2 aBC	14.1 ± 7.5 aA
Constant	7.8 ± 2.0 aB	7.1 ± 2.4 aB	7.2 ± 2.3 aC	5.7 ± 1.2 aB
CV (%)	20.67		32.12	

CV—coefficient of variation. Lowercase letters compare mean values for runoff depth and soil loss between different plots within the same rainfall pattern. Uppercase letters compare mean values within the same plot for different rainfall patterns. Mean values followed by the same letter do not differ by Tukey's test at a level of 5%.

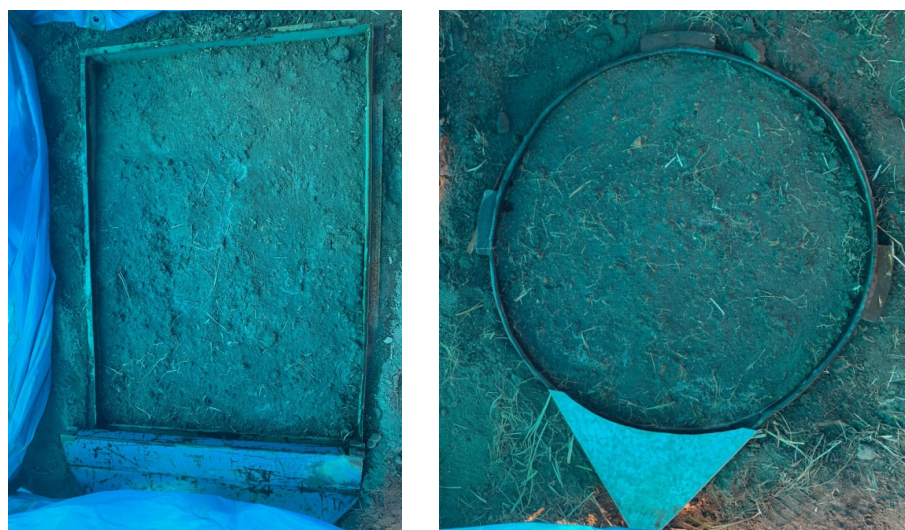


Figure 7. Experimental plots after 40 min of simulated rainfall.

4. Discussion

4.1. Precipitation Intensity, Water Use Efficiency, and the Uniformity Coefficient

In experimental research planning, knowing the WC of the rainfall simulator is important information. This helps the operator determine the required volume of water to simulate rain in the field, which is dependent on the PI and test duration.

Overall, the circular plot had a higher precipitation intensity (PI) as the *InfiAsper* water jet's wetting area tended to form a circular spray pattern. As mentioned earlier, the *InfiAsper* simulator features two conical nozzles, and as a result of the disk rotation, more water is deposited in the center of the plot, particularly at lower rotation speeds. WUE is impacted by both WC and PI. The rectangular plot generated a higher WUE due to its larger longitudinal dimension, while the circular plot, with a smaller area, received less rainfall depth, leading to a lower WUE for the plot.

Iserloh et al. [11] evaluated 13 rainfall simulators and found a range from 0.49 to 3.24 L min⁻¹ and from 4.2% to 49.3% for WC and WUE, respectively. From the equipment evaluated by the authors, the simulators from Almeria (AL) and Valencia (VA), with circular collecting plots and an area of 0.283 and 0.246 m², showed the greatest water use efficiency, of 49.3% and 42.95%, respectively, with a water consumption of 0.49 L min⁻¹ for a PI of 51 mm h⁻¹. These results differ from those found in the present study, possibly due to the differences in the types of spray nozzles (Veejet 80.150—*InfiAsper*, Hardi 4680–10E—Almeria, Hardi 1553 12—Valencia), experimental plots, and rainfall intensity.

Among the 13 simulators evaluated by [11], the CU ranged from 60.6% to 97.8%, with the highest coefficient obtained for the simulator developed at the University of Zaragoza. However, its circular collecting plot has an area of only 0.212 m², favoring greater uniformity of rainfall. In studies to determine the runoff and loss of sediment in different types of soil, the CU of the rainfall applied by a simulator developed by [31,32] was 97.8% at a rainfall intensity of 52.5 mm h⁻¹ in a circular collecting plot with an area of 0.21 m² [33]. Table 2 shows that CU reached 90.3% for a PI of 75.7 mm h⁻¹, using a circular plot with an area greater than that used by the aforementioned authors. Therefore, the shape and area of the plot are related to the better uniformity of the simulated rainfall.

4.2. Characterization of the Rainfall Patterns

Knowing the relationship between the shutter disk rotation and the respective PI value, the rainfall pattern can be configured with different combinations of intensity, duration, and depth. It is worth mentioning that *InfiAsper* was developed to simulate rainfall with constant PI [16]. The peak PI occurring throughout the rainfall is characteristic of the pattern, as described by [15]. Considering the constant pattern, the PI was kept at 45 mm h⁻¹ to provide the same rainfall depth as those with the other patterns.

4.3. Spatial Distribution of the Precipitation Intensity

The patterns were designed to ensure that all simulated rainfall had similar characteristics (Figure 4). Thus, most of the rainfall events had a PI of less than 50 mm h⁻¹, but with less variation between collectors in the circular plot (Figure 5), suggesting better results for uniformity than the rectangular plot (Table 3). According to [34], this variability may be due to the design of the collecting plot and the characteristics of the rainfall simulator.

4.4. Water and Soil Losses

Overall, portable simulators have runoff collection plots with previously predefined sizes and shapes based on the operational characteristics of the equipment. Therefore, it is not common to carry out studies comparing experimental plots for the same type of rainfall simulator.

Higher CU values were obtained in the circular plot, but this difference did not provide expressive differences in runoff and soil loss, except for simulated rainfall with the advanced pattern (AV). Due to the smaller longitudinal dimension of the circular plot and the occurrence of the PI peak (110.0 mm h⁻¹) a few minutes after the onset of rain (Figure 4),

water accumulation at the outlet was greater and faster [35]. Furthermore, the smaller area of the circular plot (0.5 m^2) may also have favored higher runoff, particularly for the IN and AV patterns. Neumann et al. [36] reported that the plot shape plays a significant role in discussions related to surface runoff and soil loss as it can potentially affect the interface between the soil surface and the collecting funnel. For instance, they found a surface runoff 30% higher in experimental plots with 1.0 m^2 than 8.0 m^2 , considering the same IP.

Although the mean precipitation intensity of 45 mm h^{-1} applied is the same for the different rainfall patterns, the peak intensity influences runoff and the soil erosion process. On the other hand, the constant pattern (CT) provided the lowest water and soil losses (Table 4), decreasing runoff by 49.6% (rectangular plot) and soil loss by 73.0% (circular plot), a value close to that obtained by [37]. Unfortunately, most simulators do not allow PI variation during rainfall application [13], making it impossible to apply rainfall that can more realistically reproduce the natural process of soil loss [22].

The greater soil loss and surface runoff provided by the AV pattern in a circular plot may also be related to the physical characteristics and the granulometric composition of the soil in the experimental area: an Acrisol with the presence of a textured B horizon (Bt), where the greatest accumulation of clay can be found (520 g kg^{-1} at a depth of 51–92 cm) (Table 1). The Bt horizon acts to limit water infiltration and drainage, favoring surface runoff and soil loss [38]. In addition, the high bulk density (1.64 g cm^{-3}) and low porosity (31.1%) in the surface horizon of this Acrisol may be the result of the superficial sealing of the soil particles, especially the fine sand, which causes dispersion and clogging of the pores, reducing water infiltration into the soil and, consequently, increasing the surface runoff.

In the rectangular plot, runoff and soil loss were higher in the IN and DL patterns, reaching, respectively, an average of 1.9 and 1.7 times greater than the values obtained in the AV pattern. A similar effect was obtained by [10] using the same rainfall simulator, but in soil with a higher clay content in the surface layers. In general, simulated rainfall under the DL pattern tends to provide higher rates of runoff and soil loss, mainly due to the prolonged period of moisture that the soil is exposed to before the peak rainfall intensity [39]. However, the results obtained with simulated rainfall cannot be easily compared due to the significant differences that exist between the rainfall simulators, such as plot size and shape, type of nozzles, as well as the size and height of the raindrops [40]. In addition, soil characteristics are also paramount in understanding the erosion process. Alavinia et al. [41] conducted an evaluation of the impact of rainfall patterns on soil erosion using a rectangular, small-scale plot filled with sandy-textured soils. The authors observed greater runoff and soil loss in the “Decreasing” and “Increasing-decreasing” patterns, which is similar to the effect observed in the circular plot in our study.

We used a rainfall simulator that meets all the criteria related to the uniformity of distribution, average diameter, terminal velocity, and kinetic energy of drops that are consistent with natural rainfall, as described by [21]. While we acknowledge that our findings enhance our knowledge of surface runoff and soil erosion processes by using rainfall simulators, we cannot consider them conclusive. It is crucial to perform future studies of precipitation patterns in experimental plots with varied shapes and sizes in different soil classes and conditions of land use and land cover.

5. Conclusions

In this study, we evaluate the operational characteristics of the *InfiAsper* rainfall simulator for different shapes of the experimental plot and its influence on soil and water loss under rainfall patterns. Rectangular experimental plots of 0.70 m^2 ($1.0 \times 0.7 \text{ m}$) and circular plots of 0.50 m^2 were evaluated in laboratory and field tests. The use of a circular plot provided greater uniformity in relation to a rectangular plot and greater PI with shutter-disk rotations below 700 rpm. From the calibration curves, rains with different patterns simulated by *InfiAsper* presented a uniformity coefficient above 83% for the circular plot and 78.2% for the rectangular plot. The soil erosion varied as a function of the precipitation patterns and, to a lesser extent, according to the shape of the experimental plot. However,

in the advanced pattern, runoff and soil loss were 2.1 and 3.5 times greater when using a circular plot. The greater longitudinal length of the rectangular plot favored the formation of small furrows throughout the simulated rainfall with IN and DL, providing higher average values of runoff (13.1 mm) and soil loss (13.6 g m^{-2}). Regardless of the plot format, the CT pattern provided the lowest runoff and soil loss. Despite the greater uniformity measured in the circular plot, rainfall-simulated tests must be carried out by *InfiAsper* in other soil classes and conditions of use and cover under different shapes associated with rainfall patterns.

Author Contributions: Conceptualization, A.S.A., D.F.d.C. and N.S.; methodology, A.S.A., D.F.d.C. and N.S.; validation, A.S.A., D.F.d.C. and N.S.; formal analysis, A.S.A., P.M.S.M., D.F.d.C. and N.S.; investigation, A.S.A., P.M.S.M., D.F.d.C. and N.S.; resources, D.F.d.C. and N.S.; data curation, A.S.A., P.M.S.M. and N.S.; writing—original draft preparation, A.S.A., P.T.S.d.O., D.F.d.C. and N.S.; writing—review and editing, A.S.A., P.T.S.d.O. and D.F.d.C.; supervision, D.F.d.C.; project administration, D.F.d.C.; funding acquisition, D.F.d.C. All authors have read and agreed to the published version of the manuscript.

Funding: This research was funded by the Conselho Nacional de Desenvolvimento Científico e Tecnológico—Brasil (CNPq) (Processes 422394/2018-1; 309752/2020-5, and it was also financed in part by the Coordenação de Aperfeiçoamento de Pessoal de Nível Superior—Brasil (CAPES)—Finance Code 001.

Institutional Review Board Statement: Not applicable.

Informed Consent Statement: Not applicable.

Data Availability Statement: Not applicable.

Acknowledgments: We would like to thank the Federal Rural University of Rio de Janeiro, specifically the PPGA-CS and GPASSA.

Conflicts of Interest: The authors declare no conflict of interest.

References

1. Abudi, I.; Carmi, G.; Berliner, P. Rainfall simulator for field runoff studies. *J. Hydrol.* **2012**, *454–455*, 76–81. [[CrossRef](#)]
2. Carvalho, D.F.; Eduardo, E.N.; Almeida, W.S.; Santos, L.A.F.; Alves Sobrinho, T. Water erosion and soil water infiltration in different stages of corn development and tillage systems. *Rev. Bras. Eng. Agrícola Ambient.* **2015**, *19*, 1072–1078. [[CrossRef](#)]
3. Zhao, L.; Hou, R.; Wu, F.; Keesstra, S. Effect of soil surface roughness on infiltration water, ponding and runoff on tilled soils under rainfall simulation experiments. *Soil Tillage Res.* **2018**, *179*, 47–53. [[CrossRef](#)]
4. Kabelka, D.; Kincl, D.; Janeček, M.; Vopravil, J.; Vráblik, P. Reduction in soil organic matter loss caused by water erosion in inter-rows of hop gardens. *Soil Water Res.* **2019**, *14*, 172–182. [[CrossRef](#)]
5. Kavian, A.; Mohammad, M.; Cerdà, A.; Fallah, M.; Abdollahi, Z. Simulated raindrop's characteristic measurements. A new approach of image processing tested under laboratory rainfall simulation. *Catena* **2018**, *167*, 190–197. [[CrossRef](#)]
6. Wang, B.; Steiner, J.; Zheng, F.; Gowda, P. Impact of rainfall pattern on interrill erosion process. *Earth Surf. Process. Landf.* **2017**, *42*, 1833–1846. [[CrossRef](#)]
7. Marques, V.S.; Ceddia, M.B.; Antunes, M.A.H.; Carvalho, D.F.; Anache, J.A.A.; Rodrigues, D.B.B.; Oliveira, P.T.S. USLE K-Factor Method Selection for a Tropical Catchment. *Sustainability* **2019**, *11*, 1840. [[CrossRef](#)]
8. Falcão, K.S.; Panachuki, E.; Monteiro, F.N.; Menezes, R.S.; Rodrigues, D.B.B.; Sone, J.S.; Oliveira, P.T.S. Surface runoff and soil erosion in a natural regeneration area of the Brazilian Cerrado. *Int. Soil Water Conserv. Res.* **2020**, *8*, 124–130. [[CrossRef](#)]
9. Munster, C.L.; Taucer, P.I.; Wilcox, B.P.; Porter, S.C.; Richards, C.E. An approach for simulating rainfall above the tree canopy at the hillslope scale. *Trans. ASABE* **2006**, *49*, 915–942. [[CrossRef](#)]
10. Carvalho, D.F.; Macedo, P.M.S.; Pinto, M.F.; Almeida, W.S.; Schultz, N. Soil loss and runoff obtained with customized precipitation patterns simulated by *InfiAsper*. *Int. Soil Water Conserv. Res.* **2022**, *10*, 407–413. [[CrossRef](#)]
11. Iserloh, T.; Ries, J.B.; Arnáez, J.; Boix-Fayos, C.; Butzen, V.; Cerdà, A.; Echeverría, M.T.; Fernández-Gálvez, J.; Fister, W.; Geißler, C.; et al. European small portable rainfall simulators: A comparison of rainfall characteristics. *Catena* **2013**, *110*, 100–112. [[CrossRef](#)]
12. Mhaske, S.N.; Pathak, K.; Basak, A. A comprehensive design of rainfall simulator for the assessment of soil erosion in the laboratory. *Catena* **2019**, *172*, 408–420. [[CrossRef](#)]
13. Sousa, S.F.; Mendes, T.A.; Siqueira, E.Q. Development and calibration of a rainfall simulator for hydrological studies. *Rev. Bras. Recur. Hídric.* **2017**, *22*, e59. [[CrossRef](#)]
14. Dunkerley, D. The case for increased validation of rainfall simulation as a tool for researching runoff, soil erosion, and related processes. *Catena* **2021**, *202*, 105283. [[CrossRef](#)]

15. Flanagan, D.C.; Foster, G.R.; Moldenhauer, W.C. Storm patterns effect on infiltration, runoff, and erosion. *Trans. ASAE* **1988**, *31*, 414–420. [[CrossRef](#)]
16. Alves Sobrinho, T.; Gomez-Macpherson, H.; Gomez, J.A. A portable integrated rainfall and overland flow Simulator. *Soil Use Manag.* **2008**, *24*, 163–170. [[CrossRef](#)]
17. Panachuki, E.; Santos, M.A.N.; Pavei, D.S.; Alves Sobrinho, T.; Silva, M.A.C.; Montanari, R. Soil and water loss in Ultisol of the Cerrado-Pantanal Ecotone under different management systems. *Afr. J. Agric. Res.* **2015**, *10*, 926–932. [[CrossRef](#)]
18. Almeida, W.S.; Panachuki, E.; Oliveira, P.T.S.; Silva, R.M.; Alves Sobrinho, T.; Carvalho, D.F. Effect of soil tillage and vegetal cover on soil water infiltration. *Soil Tillage Res.* **2018**, *175*, 130–138. [[CrossRef](#)]
19. Alves, M.A.B.; Souza, A.P.; Almeida, F.T.; Hoshide, A.K.; Araujo, H.B.; Silva, A.F.; Carvalho, D.F. Influence of land use and crop cover on soil erosion in agricultural frontier areas in the Cerrado-Amazon ecotone, Brazil. *Sustainability* **2023**, *15*, 4954. [[CrossRef](#)]
20. Morin, J.; Goldberg, D.; Seginer, I. A rainfall simulator with rotating disk. *Trans. ASAE* **1967**, *10*, 74–77. [[CrossRef](#)]
21. Macedo, P.M.S.; Pinto, M.F.; Alves Sobrinho, T.; Schultz, N.; Coutinho, T.A.R.; Carvalho, D.F. A Modified portable rainfall simulator for soil erosion assessment under different rainfall patterns. *J. Hydrol.* **2021**, *596*, 126052. [[CrossRef](#)]
22. Nielsen, K.T.; Moldrup, P.; Thorndahl, S.; Nielsen, J.E.; Duus, L.B.; Rasmussen, S.H.; Uggerby, M.; Rasmussen, M.R. Automated rainfall simulator for variable rainfall on urban green areas. *Hydrol. Process.* **2019**, *33*, 3364–3377. [[CrossRef](#)]
23. Green, D.; Pattison, I. Christiansen uniformity revisited: Re-thinking uniformity assessment in rainfall simulator studies. *Catena* **2022**, *217*, 106424. [[CrossRef](#)]
24. Christiansen, J.E. *Irrigation by Sprinkling*; California Agricultural Experiment Station: Berkeley, CA, USA, 1942.
25. Dunkerley, D. Rain event properties in nature and in rainfall simulation experiments: A comparative review with recommendations for increasingly systematic study and reporting. *Hydrol. Process* **2008**, *22*, 4415–4435. [[CrossRef](#)]
26. Kinnell, P.I.A. A review of the design and operation of runoff and soil loss plots. *Catena* **2016**, *145*, 257–265. [[CrossRef](#)]
27. Amore, E.; Modica, C.; Nearing, M.A.; Santoro, V.C. Scale effect in USLE and WEPP application for soil erosion computation from three Sicilian basins. *J. Hydrol.* **2004**, *293*, 100–114. [[CrossRef](#)]
28. IUSS Working Group WRB. *World Reference Base for Soil Resources. International Soil Classification System for Naming Soils and Creating Legends for Soil Maps*, 4th ed.; International Union of Soil Sciences (IUSS): Vienna, Austria, 2022.
29. Santos, H.G.; Jacomine, P.K.T.; Anjos, L.H.C.; Oliveira, V.A.; Lumbreras, J.F.; Coelho, M.R.; Almeida, J.A.; Cunha, T.J.F.; Oliveira, J.B. *Brazilian Soil Classification System*, 5th ed.; National Center for Soil Research: Rio de Janeiro, Spain, 2018; pp. 287–306.
30. Ferreira, D. Sisvar: A computer statistical analysis system. *Ciênc. Agrotecnol.* **2011**, *35*, 1039–1042. [[CrossRef](#)]
31. Cerdà, A.; Ibáñez, S.; Calvo, A. Design and operation of a small and portable rainfall simulator for rugged terrain. *Soil Technol.* **1997**, *11*, 163–170. [[CrossRef](#)]
32. Lasanta, T.; García-Ruiz, J.M.; Pérez-Rontomé, C.; Sancho-Marcén, C. Runoff and sediment yield in a semi-arid environment: The effect of land management after farmland abandonment. *Catena* **2000**, *38*, 265–278. [[CrossRef](#)]
33. León, J.; Echeverría, M.; Badía, D.; Martí, C.; Álvarez, C. Effectiveness of wood chips cover at reducing erosion in two contrasted burnt soils. *Z. Fur Geomorphol. Suppl.* **2013**, *57*, 27–37. [[CrossRef](#)]
34. Iserloh, T.; Fister, W.; Seeger, M.; Willger, H.; Ries, J. A small portable rainfall simulator for reproducible experiments on soil erosion. *Soil Tillage Res.* **2012**, *124*, 131–137. [[CrossRef](#)]
35. Mayerhofer, C.; Meißl, G.; Klebinder, K.; Kohl, B.; Markart, G. Comparison of the results of a small-plot and a large-plot rainfall simulator—Effects of land use and land cover on surface runoff in Alpine catchments. *Catena* **2017**, *156*, 184–196. [[CrossRef](#)]
36. Neumann, M.; Kavka, P.; Devátý, J.; Stašek, J.; Strouhal, L.; Tejkl, A.; Kubínová, R.; Rodrigo-Comino, J. Effect of plot size and precipitation magnitudes on the activation of soil erosion processes using simulated rainfall experiments in vineyards. *Front. Environ. Sci.* **2022**, *10*, 949774. [[CrossRef](#)]
37. Parsons, A.J.; Stone, P.M. Effects of intra-storm variations in rainfall intensity on interrill runoff and erosion. *Catena* **2006**, *67*, 68–78. [[CrossRef](#)]
38. Li, X.; Chang, S.X.; Salifu, K.F. Soil texture and layering effects on water and salt dynamics in the presence of a water table: A review. *Environ. Rev.* **2014**, *22*, 1–10. [[CrossRef](#)]
39. Dunkerley, D. Effects of rainfall intensity fluctuations on infiltration and runoff: Rainfall simulation on dry land soils, Fowlers Gap, Australia. *Hydrol. Process.* **2012**, *26*, 2211–2224. [[CrossRef](#)]
40. Schindler Wildhaber, Y.; Bänninger, D.; Burri, K.; Alewell, C. Evaluation and application of a portable rainfall simulator on subalpine grassland. *Catena* **2012**, *91*, 56–62. [[CrossRef](#)]
41. Alavinia, M.; Saleh, F.N.; Asadi, H. Effects of rainfall patterns on runoff and rainfall-induced erosion. *Int. J. Sediment Res.* **2019**, *34*, 270–278. [[CrossRef](#)]

Disclaimer/Publisher's Note: The statements, opinions and data contained in all publications are solely those of the individual author(s) and contributor(s) and not of MDPI and/or the editor(s). MDPI and/or the editor(s) disclaim responsibility for any injury to people or property resulting from any ideas, methods, instructions or products referred to in the content.